Journal Name

RSCPublishing

COMMUNICATION

Switching Intermolecular Interactions by Confinement in Carbon Nanotubes†

Cite this: DOI: 10.1039/x0xx00000x

T. W. Chamberlain,[a]* M. A. Lebedeva,[a] W. Abuajwa,[a] M. Suyetin,[a,b] W. Lewis,[a] E. Bichoutskaia,[a] M. Schröder[a] and A. N. Khlobystov[a,c]

Received 00th January 2012,
Accepted 00th January 2012

DOI: 10.1039/x0xx00000x

www.rsc.org/

The encapsulation of trityl-functionalised C_{60} molecules inside carbon nanotubes drastically affects the intermolecular interactions for this species. Whilst the orientations of molecules in the crystal are often controlled by thermodynamics, the molecular orientations in nanotubes are a result of kinetic control imposed by the mechanism of entry into and encapsulation within the nanotube.

The development of a new methodology to control the specific orientations and packing of molecules within supramolecular arrays is a challenge that is crucial for the advancement of molecular nanotechnology. C_{60} and the family of fullerenes have unique physical and chemical properties such as light absorption extending throughout the entire UV-vis spectrum, the ability to contain spin carriers, effective electron accepting ability and superconductivity upon doping with alkali metals.[1] They thus represent attractive functional building blocks for molecular assemblies and supramolecular arrays. C_{60}, however, offers only non-directional van der Waals interactions to external species. A wide range of hosts designed to maximise these potentially strong van der Waals interactions have been used to bind or trap C_{60} including calix[n]arenes,[2] cyclic paraphenyleneacetylenes,[3] cyclotriveratrylenes,[4] π-extended tetrathiafulvalenes,[5] porphyrins,[6] and cyclothiophenes.[7] Assemblies on surfaces,[8] and in the internal channels of single-walled carbon nanotubes (SWNTs)[9,10] to form 2D and 1D arrays of fullerenes, respectively, have also been used to interact with and order molecular C_{60}.

An alternative approach to develop directional and controlled binding of C_{60} is to utilise the rich library of fullerene chemistry now available to attach a functional group to the side of the fullerene cage. Functionalisation of the carbon cage can be used to introduce structurally rigid groups which direct the molecules into 1D chains,[11] or groups with functional properties such as tetrathiafulvalene,[12] and porphyrins,[13] crown ethers,[14] salen[15] or bipyridine[16] ligands which can exploit the coordination geometry of a metal centre to control intermolecular interactions and the shape of the resultant array of fullerenes.

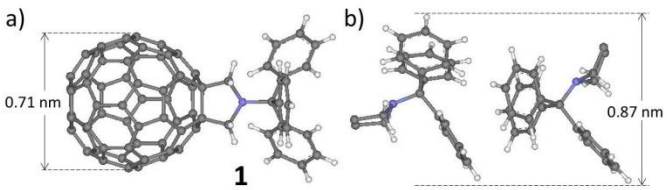

Figure 1. a) Functionalised fullerene **1** and b) the phenyl embrace formed between trityl groups of two molecules of **1** (the fullerene cages have been omitted for clarity). The distances shown are the approximate diameters of the fullerene cage of **1** and the trityl-trityl phenyl embrace formed by two molecules of **1**.

The structure of a fullerene-based molecular array is the result of the fine balance between attractive fullerene to fullerene and fullerene to host or to functional group interactions. We demonstrate herein that the assembly of fullerene molecules in the crystal is affected by phenyl embraces of an appended trityl group which disrupts inter-fullerene interactions and assists the orientation of the fullerene molecules. We find that nanoscale confinement of functionalised fullerenes switches these intermolecular orientations to a mode that is quite different to that observed within the single crystal structure due to the mechanism of encapsulation within carbon nanotubes.

The functionalised fullerene **1** (Figure 1) incorporating a triphenylmethyl (trityl) group attached to C_{60} via a pyrrolidine ring was synthesised according to a method previously reported by us.[17] Crystals of **1** suitable for single crystal X-ray diffraction analysis were grown by slow diffusion of diethyl ether into a saturated solution of **1** in CS_2 over the course of a few weeks. Detailed analysis of the single crystal X-ray structure of **1** reveals three types of supramolecular interactions that direct the packing of the molecules of **1** in the solid state.

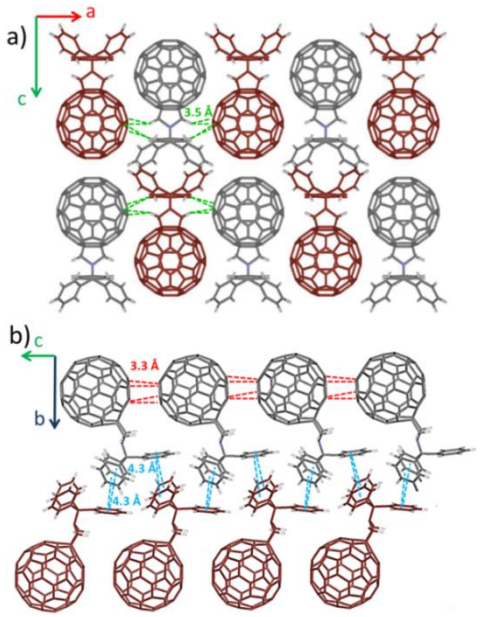

Figure 2. a) View of the crystal structure of **1** along the *b* axis showing the projection of the molecules in the *ac* plane forming a pseudo-hexagonal packing motif of fullerene cages, highlighting fullerene-trityl C-H….π interactions (green dashed lines); b) view of the crystal structure of **1** along the *a* axis showing the edge-to-face interactions between the neighbouring trityl groups (blue dashed lines) and fullerene-fullerene short contacts (red dashed lines). Molecules of **1** in different corrugated layers are shown in grey and red to emphasise the distortion from hexagonal packing.

The trityl groups interact with each other such that the two edges of one of the phenyl rings of the trityl group interact with the faces of the two phenyl rings of the neighbouring trityl group approaching at a distance of 4.3 Å (Figure 2b). The remaining phenyl ring is then engaged in the same kind of interaction with the trityl group of a neighbouring molecule thus forming a 1D chain (Figure 2b, blue dashed lines). The central sp^3 carbon atoms of the two interacting trityl groups approach at a distance of 7.2 Å and the two C-N bonds between trityl and pyrrolidine groups form an angle of 147.7° This type of phenyl embrace interaction is not uncommon and has been observed previously for non-fullerene systems.[18] Each trityl group also exhibits C-H…π interactions with two fullerene units at a distance of approximately 3.5 Å (Figure 2a, green dashed lines). Additionally, each of the fullerene cages also interacts with two neighbouring C_{60} units forming close contacts between the pentagonal rings on each cage with a distance of 3.3 Å (Figure 2b, red dashed lines). As a result of these interactions the single crystal X-ray structure of **1** exhibits stacking of the molecules in columns in the [010] direction (along the *b* crystallographic axis) to form a pseudo-hexagonal packing motif (Figure 2a) similar to the hexagonal close packing of the molecules in the C_{60} crystal.[19] The solid state structure shows a crystallographic mirror plane of symmetry, with the trityl groups orientated such that they predominantly face each other. Importantly, as two neighbouring trityl groups occupy a volume which is slightly bigger than a C_{60} unit (Figure 1b) this causes a slight distortion of the hexagonal packing of C_{60} units into two corrugated layers (Figure 2a, red and grey colours).

Single-walled carbon nanotubes (SWNTs) with nanometre sized diameters but up to millimetre in length provide a quasi-1D environment ideal for creating chains of molecules. The unique structures and properties of these molecular chains and the ability to

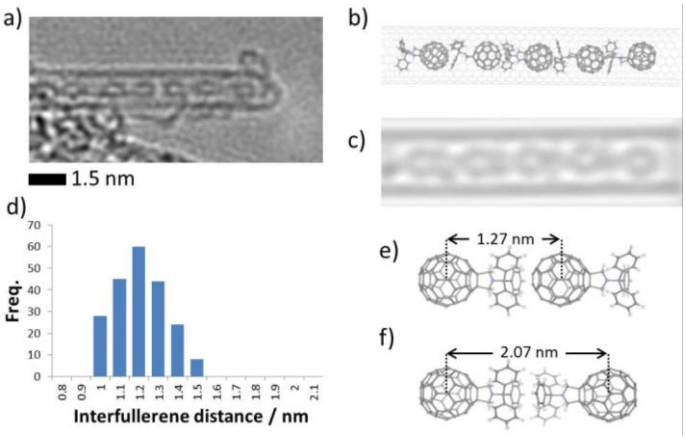

Figure 3. a) HRTEM image of 1D molecular arrays of **1**@SWNT. The slightly elongated shape of the fullerene cages is due to distortion of the functionalised cage during image acquisition caused by the electron beam[9] b, c) structural model and simulated TEM image of **1**@SWNT; d) distribution of interfullerene spacings (measured between the centres of neighbouring fullerene cages by HRTEM) in **1**@SWNT; and e, f) expected separations of two molecules of **1** in fullerene-to-trityl and trityl-to-trityl orientations respectively

manipulate and incorporate carbon nanotubes (together with any molecules encapsulated inside) into devices such as field-effect transistors (FET)[1] and modified electrodes[20] makes the design and formation of highly ordered fullerene nanotubes an important goal. As well as interacting strongly with other fullerene molecules, as observed in the crystal structure of **1**, the C_{60} cage of **1** is ideally shaped to interact with the interior of SWNTs through van der Waals interactions, the binding energy of C_{60} encapsulated inside SWNTs being measured as 288 kJ mol^{-1}.[21]

To explore this, fullerene **1** was inserted into SWNTs by immersing freshly opened nanotubes in a supersaturated solution of **1** in toluene followed by heating overnight. It has been demonstrated previously[22] that the presence of clusters of fullerene molecules within such supersaturated solutions enables the molecules to enter SWNTs with an internal diameter of 1.4 nm, displacing any solvent that might reside within the SWNT. This avoids the detrimental influence of solvent on the nanotube filling process and prevents solvent molecules from disrupting the ordering of the molecules within the nanotube cavity in such a way that the molecules of **1** can be considered to be tightly packed in the nanotube cavity.[22] The resultant fullerene arrays of **1** in SWNT were analysed using high resolution transmission electron microscopy (HRTEM) with the imaging conditions (low energy and dose of the e-beam) set to minimise the knock-on damage that commonly occurs to molecular species on exposure to the electron beam. Imaging at high magnification reveals that the nanotube cavities are filled with ordered arrays of fullerenes (Figure 3a and ESI file). Fullerene cages can be clearly observed as elliptically distorted circles between the SWNT sidewalls, thus unambiguously verifying the presence of these guest molecules. Consideration of the average centre-to-centre separation of the fullerene cages in the **1**@SWNT structures, 1.21 ± 0.12 nm, as measured from direct-space HRTEM image analysis, reveals that the molecules almost exclusively adopt a fullerene-to-trityl orientation (Figure 3e) leading to significant C_{60}…trityl interactions inside the nanotube. Fullerene-to-fullerene and trityl-to-trityl orientations would result in 1.00 nm and 2.07 nm separations

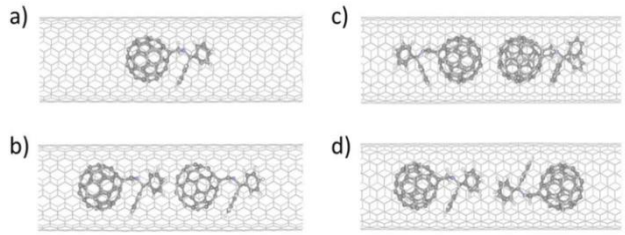

Figure 4. Lowest energy configurations of **1** inside a (10,10)SWNT (d_{NT} = 1.36 nm), for a) an individual **1** molecule, and two molecules of **1** arranged in b) fullerene-to-trityl, c) fullerene-to-fullerene and d) trityl-to-trityl orientations.

between fullerene cages, respectively. Significantly, analysis of the the average centre-to-centre separation in **1**@SWNT reveals that trityl-to-trityl orientations requiring a fullerene to fullerene separation of 2.07nm (Figure 3f), and which are significant in the solid state structure, appear to be absent when **1** is bound within SWNTs. Rather , in **1**@SWNT the fullerene-to-trityl packing motif becomes dominant. Although it cannot be fully discounted from the images that some fullerene-to-fullerene interactions (expected separation of 1.00 nm) might occur due to packing and/or lateral movement of the substrates within the nanotube, indeed the abundance of larger fullerene separations (1.4-1.5 nm) are attributed to discrepancies in packing and/or movement of fullerene-to-trityl orientated molecules, the absence of concomitant trityl-to-trityl interactions requiring 2.07 nm separations suggests that this not a major pathway of packing within the nanotube. Interaction between fullerene units and aryl groups is a common motif in supramolecular assemblies of fullerenes with different aromatic molecules.[23,24] Thus, the removal of fullerene-fullerene and trityl-trityl interactions with neighbouring molecules, which dominate the molecular packing in the solid state crystal, can be ascribed to the confinement imposed by the 1D channel of the SWNT.

To investigate the mechanisms for the switching of intermolecular interactions in our experiments, theoretical simulations were performed for the three different potential orientations of **1** inside a (10,10)SWNT of diameter 1.36 nm, which is close to the mean nanotube diameter of the SWNT employed in our experiments (Figure 4, Table 1).

Table 1. Calculated binding energies and inter-molecular interaction energies for different orientations of pairs of **1** inside a (10,10)SWNT.

Orientation	**Total binding energy / kJ mol^{-1}**	**Inter-molecular interaction energy / kJ mol^{-1}**
Individual molecule	401.90	-
Fullerene-to-trityl	410.36	-8.46
Fullerene-to-fullerene	412.80	-10.19
Trityl-to-trityl	402.94	-1.04

Calculations reveal that addition of the trityl group to the fullerene cage results in a total binding energy upon encapsulation of 404 kJ mol^{-1} compared with a binding energy of 288 kJ mol^{-1} for C_{60}@SWNT.[20] This increase in binding energy of 116 kJ mol^{-1} compared to free C_{60}, is attributed to the greater surface area of **1** due to the aromatic phenyl groups of the trityl moiety, leading to higher surface of contact with SWNT and thus stronger total van der Waals

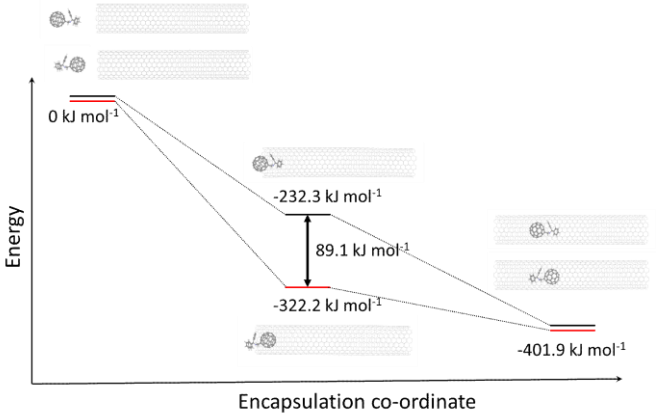

Figure 5. Calculated energies for encapsulation of **1** into a (10,10)SWNT for two different orientations of **1**: fullerene cage first (red) and trityl group first (black). A significant difference in energy of ~90 kJmol^{-1} is observed for the critical encapsulation step depending upon the orientations of **1** when it becomes engaged in interactions with the nanotube cavity (centre of diagram). **1** prefers to enter the nanotube with the fullerene cage first, and this determines the preferential orientation of 1 inside nanotubes as observed by HRTEM imaging. Thus, two fullerenes entering from opposite ends of the nanotube would results in a fullerene to fullerene interaction

interactions. The lowest energy configuration of two molecules of **1** in a trityl-trityl orientation (Figure 4d) confirms that there is sufficient room within the confines of the nanotube for trityl-trityl interactions. However, the geometry of such an interaction is distinctly different in the SWNT to that in the solid-state crystal structure with a wider angle of 179.9° observed between the two (trityl)C-N bonds of the two embracing trityl groups compared to 147.7° in the crystal structure of free 1, in which this angle is more acute due to competing intermolecular interactions.

Detailed comparison of the stabilities of the different orientations within the nanotube show only small differences in energy of below 10 kJ mol^{-1}. Considering that compound **1** is inserted into the nanotubes at elevated temperatures (80 °C), the three orientations (Figure 4c-d) are expected to form with equal probability. However, HRTEM analysis reveals non-random orientations of **1** in nanotubes, with the majority of molecules arranged in a fullerene-to-trityl fashion within molecular chains (Figure 4b). Such an orientation is not observed in the bulk crystal (Figure 2) and therefore must be a result of nanoscale confinement, the origin of which, however, cannot be explained by solely considering the thermodynamic stability. It should be noted that functionalised fullerene molecules preferentially organised inside SWNT in a fullerene-to-functional group configuration have been observed previously; however, no explanation for this has been suggested.[10,25,26]

Consideration of the key steps of the mechanism of encapsulation of **1** using molecular mechanics simulations (see ESI for details) shows a significant difference in energy (~90 kJ mol^{-1}) for the critical step of insertion, when the molecule becomes engaged in interactions with the nanotube cavity; this varies for different orientations of **1** (middle diagram, Figure 5). The pathway when the fullerene cage of **1** enters the nanotube first leads to a rapid increase in energy during encapsulation due to the size and shape cooperativity between the fullerene cage and the cylindrical cavity of the nanotube. In contrast, along the pathway where the trityl group enters the nanotube first, the initial increase in binding energy is significantly lower. Upon complete encapsulation of the molecule into the confines of the

nanotube the encapsulation energies of both orientations are equal. It is important to emphasise that that orientations cannot change once the molecules are inside of the nanotubes as any rotation of molecule **1** perpendicular to the nanotube axis is forbidden due to the steric bulk of the trityl group. As a result, the preferential fullerene-first encapsulation mechanism leads to a uniform and ordered fullerene-to-trityl arrangement inside the SWNT as observed by HRTEM imaging. The alternative arrangement of fullerene-to-fullerene and trityl-to-trityl are thus precluded for kinetic rather than thermodynamic reasons linked to the preferred mechanism of entry of **1** into the nanotube.

Conclusions

We have demonstrated that encapsulation of molecules of a trityl-functionalised C_{60}, **1**, in nanotubes drastically affects the resultant intermolecular interactions and alters the preferred orientations of the functionalised fullerene compared to that in the solid-state crystal structure. Orientations of molecules in the crystal are predominantly controlled by thermodynamics whilst inside nanotubes they are kinetically controlled and determined by the mechanism of encapsulation. Thus, the specific orientation of molecules at the crucial step of insertion into the nanotube determines the observed intermolecular interactions inside the nanotube channel, which cannot be altered once the molecules have been encapsulated due to restricted rotation of the molecules. This offers a new and powerful method to control the arrangement of molecular chains. The functional properties of nanotubes, including electrical and spin-coherent conductance, and their unique structure, mean that nanotubes can be considered as highly suitable nanoscale vessels for organising molecular arrays, and consequently such systems can be utilised to bridge the gap between molecules and the macroworld providing materials for use in molecular based electronic and spintronic applications.

Notes and references

[a] School of Chemistry, The University of Nottingham, University Park, Nottingham, NG7 2RD, UK. Tel: +44 (0)115 9513917; Fax: +44 (0)115 9513563; E-mail: thomas.chamberlain@nottingham.ac.uk.

[b] Institute of Mechanics of Ural Branch of Russian Academy of Sciences, T. Baramzinoy Str., 34, Izhevsk, 426067, Russian Federation.

[c] Nottingham Nanotechnology & Nanoscience Centre, University of Nottingham, University Park, Nottingham, NG7 2RD, UK.

† This work was supported by the European Research Council (ERC), Engineering and Physical Sciences Research Council (EPSRC) and University of Nottingham. We thank the Nottingham Nanotechnology and Nanoscience Centre (NNNC) for access to electron microscopy facilities and High Performance Computing Facility (HPC) at the University of Nottingham for access to computing resources.

Electronic Supplementary Information (ESI) available: Additional TEM data, experimental methods and theoretical details are included. See DOI: 10.1039/c000000x/

1 S. S. Babu, H. Mohwald and T. Nakanishi, *Chem. Soc. Rev.*, 2010, 39, 4021.

2 E. M. Perez and N. Martin, *Chem. Soc. Rev.*, 2008, **37**, 1512.

3 T. Kawase, K. Tanaka, N. Fujiwara, H. R. Darabi and M. Oda, *Angew. Chem. Int. Edit.*, 2003, **42**, 1624.

4 H. Matsubara, A. Hasegawa, K. Shiwaku, K. Asano, M. Uno, S. Takahashi and K. Yamamoto, *Chem. Lett.*, 1998, 923.

5 E. M. Perez, L. Sanchez, G. Fernandez and N. Martin, *J. Am. Chem. Soc.*, 2006, **128**, 7172.

6 D. Bonifazi, H. Spillmann, A. Kiebele, M. de Wild, P. Seiler, F. Y. Cheng, H. J. Guntherodt, T. Jung and F. Diederich, *Angew. Chem. Int. Edit.*, 2004, **43**, 4759.

7 E. M. Perez and N. Martin, *Pure Appl. Chem.*, 2010, **82**, 523.

8 M. T. Raisanen, A. G. Slater, N. R. Champness and M. Buck, *Chem. Sci.*, 2012, **3**, 84.

9 A. N. Khlobystov, D. A. Britz, A. Ardavan and G. A. D. Briggs, *Phys. Rev. Lett.*, 2004, 92.

10 E. Nakamura, Angew. *Chem. Int. Edit.*, 2013, **52**, 236.

11 M. Sawamura, K. Kawai, Y. Matsuo, K. Kanie, T. Kato and E. Nakamura, *Nature*, 2002, **419**, 702.

12 G. Fernandez, E. M. Perez, L. Sanchez and N. Martin, *Angew. Chem. Int. Edit.*, 2008, **47**, 1094.

13 P. A. Liddell, D. Kuciauskas, J. P. Sumida, B. Nash, D. Nguyen, A. L. Moore, T. A. Moore and D. Gust, *J. Am. Chem. Soc.*, 1997, **119**, 1400.

14 U. Jonas, F. Cardullo, P. Belik, F. Diederich, A. Gugel, E. Harth, A. Herrmann, L. Isaacs, K. Mullen, H. Ringsdorf, C. Thilgen, P. Uhlmann, A. Vasella, C. A. A. Waldraff and M. Walter, *Chem-Eur. J.*, 1995, **1**, 243.

15 M. A. Lebedeva, T. Chamberlain, E. S. Davies, D. Mancel, B. E. Thomas, M. Suyetin, E. Bichoutskaia, M. Schröder and A. N. Khlobystov, *Chem-Eur. J.*, 2013, **19**, 11999.

16 J. Fan, Y. Wang, A. J. Blake, C. Wilson, E. S. Davies, A. N. Khlobystov and M. Schroeder, *Angew. Chem. Int. Edit.*, 2007, **46**, 8013.

17 M. A. Lebedeva, T. W. Chamberlain, M. Schröder and A. N. Khlobystov, *Tetrahedron*, 2012, **68**, 4976.

18 I. Dance and M. Scudder, *Chem-Eur. J.*, 1996, **2**, 481.

19 H. W. Kroto, J. R. Heath, S. C. Obrien, R. F. Curl and R. E. Smalley, *Nature*, 1985, **318**, 162.

20 R. L. McSweeney, T. W. Chamberlain, E. S. Davies, A. N. Khlobystov, *Chem. Comm.*, 2014, DOI: 10.1039/C4CC06964A.

21 H. Ulbricht, G. Moos and T. Hertel, *Phys. Rev. Lett.*, 2003, 90.

22 T. W. Chamberlain, A. M. Popov, A. A. Knizhnik, G. E. Samoilov and A. N. Khlobystov, *ACS Nano*, 2010, **4**, 5203.

23 A. L. Balch, V. J. Catalano, J. W. Lee and M. M. Olmstead, *J. Am. Chem. Soc.*, 1992, **114**, 5455.

24 M. Fedurco, M. M. Olmstead and W. R. Fawcett, *Inorg. Chem.*, 1995, **34**, 390.

25 T. W. Chamberlain, A. Camenisch, N. R. Champness, G. A. D. Briggs, S. C. Benjamin, A. Ardavan and A. N. Khlobystov, *J. Am. Chem. Soc.*, 2007, **129**, 8609.

26 T. W. Chamberlain, R. Pfeiffer, J. Howells, H. Peterlik, H. Kuzmany, B. Krautler, T. Da Ros, M. Melle-Franco, F. Zerbetto, D. Milic and A. N. Khlobystov, *Nanoscale*, 2012, **4**, 7540.

